The Astrophysical Journal, 570:373–378, 2002 May 1

TIME-DEPENDENT ASYMMETRIES IN THE ATMOSPHERE OF THE MIRA VARIABLE R TRIANGULI THROUGH INFRARED INTERFEROMETRY

R. R. Thompson,[1,2] M. J. Creech-Eakman,[1,3] and R. L. Akeson[1,4]

Received 2001 September 5; accepted 2002 January 1

ABSTRACT

We report high-resolution (<0.05 mas) angular size measurements of the Mira variable star R Tri using the Palomar Testbed Interferometer. Observations were conducted in the *K* band (2.0–2.4 μm) between the visual phases of 0.77 and 0.88, and one period later at phase 0.91. The spatial coverage of the measurements spans 40° in position angle. Three simple geometries were modeled: a uniform ellipse model and a uniform sphere with a brighter "disk" model have lower χ^2_μ than the uniform spherical disk model by factors of 5–10. For the axially symmetric models, the axis of symmetry is clustered between 20° and 35°. The position angles are roughly perpendicular to visual polarization position angles, which supports an axially symmetric source of light scattering. For the elliptical geometry, averaging the semimajor and semiminor axes throughout the data set yields an ensemble average angular diameter of 5.22 ± 0.30 mas; the ensemble average axial ratio of $2a/2b = 0.75$ is similar to that previously determined for other Mira and semiregular variable stars.

Subject headings: infrared: stars — stars: AGB and post-AGB — stars: atmospheres — stars: fundamental parameters — stars: individual (R Trianguli) — techniques: interferometric

1. INTRODUCTION

Asymptotic giant branch (AGB) and post-AGB stars are characterized by their extended stellar atmospheres. Departures from spherical symmetry of these outer atmospheres may occur as a result of stellar rotation, nonradial pulsation, and stellar hot spots due to large-scale convection of the outer layers. Asymmetries in the outer atmospheres and circumstellar envelopes have been reported in red giants, Mira variables, and Mira-like stars using various techniques. Spatially resolved studies of α Ori in the mid-infrared have found departures from spherical symmetry of the surrounding dust shell (Weiner et al. 2000). Asymmetries of a stellar atmosphere using a nonredundant pupil-masking method have been seen in the oxygen-rich Mira R Leo (Tuthill et al. 1994). Using the same technique, no significant departures from spherical symmetry were found in the near-infrared (NIR) angular size of the oxygen-rich Mira R Aqr; however, long baseline interferometry in the mid-infrared, which traces different circumstellar material, shows a substantial effect in this respect (Tuthill et al. 2000). (For clarity, Michelson stellar interferometers measure visibilities of the two-dimensional projection of a three-dimensional object.) Although limited to only the largest angular sizes, direct imaging using the *Hubble Space Telescope* (*HST*) has shown departures from spherical symmetry in the outer atmosphere of the oxygen-rich Mira *o* Cet (Karovska 1999).

A number of studies have been conducted that attempt to fit elliptical models to the measured visibilities of other AGB and post-AGB stars. Hofmann et al. (2000), using speckle masking on the 6 m Smithsonian Astrophysical Observatory telescope, found the major and minor diameters of the oxygen-rich Mira R Cas using uniform elliptical disk models. Corresponding axial ratios ($2b/2a$) in the visible were between 0.70 and 0.87. No asymmetries were detected at 1040 nm, and a lower limit to the axial ratio was placed at 0.9. Lattanzi et al. (1997) used the Fine Guidance Sensor on *HST* to measure the diameters of R Leo and the semiregular pulsator W Hya, with respective axial ratios of 0.90 ± 0.03 and 0.84 ± 0.03 in the visible.

This paper focuses on the previously unremarkable Mira variable R Tri. This star is classified as oxygen-rich, with spectral types varying during its pulsation cycle (266 days) ranging M4e–M8e III. According to the *IRAS* Low Resolution Spectrometer catalog (Olnon et al. 1986), R Tri is classified as "1n" and was determined to be featureless in the 8–21 μm region. After removal of the stellar spectrum, however, Sloan & Price (1998) classify R Tri as a star with modest silicate and oxygen-rich dust emission ("SE3"). Additionally, as is common with oxygen-rich Mira stars, oxygen-rich compounds have been detected at and about the stellar atmosphere. Castelaz et al. (2000) detected ZrO, VO, and TiO using spectroscopy in the visual, and Benson et al. (1990) detected circumstellar H_2O and SiO masers. Short-period Mira variables ($P < 300$ days) are thought to be second-ascent red giants with low mass loss (10^{-7} $M_\odot$ yr^{-1}); Jura (1994) points out that the short-period Mira R Tri has a mass loss of 1.1×10^{-7} $M_\odot$ yr^{-1}. Jura also notes that, on average, short-period Mira variables tend to reside in the galactic halo; however, R Tri belongs to the "extended/thick disk" population. Given R Tri's high proper motion ($\simeq$40 mas yr^{-1}), it appears this star is passing through the Orion arm from the Galactic halo.

Interferometric measurements of Mira variables are important to gaining a better understanding of these evolved, pulsating stars. With the dedicated observational program of Mira variables at the Palomar Testbed Interfer-

[1] Jet Propulsion Laboratory, California Institute of Technology, MS 171-113, 4800 Oak Grove Drive, Pasadena, CA 91109-8099;thompson@huey.jpl.nasa.gov.

[2] University of Wyoming, Department of Physics and Astronomy, Laramie, WY 82071.

[3] California Institute of Technology, 1200 East California Boulevard, Pasadena, CA 91125.

[4] Infrared Processing and Analysis Center, California Institute of Technology, MS 100-22, 700 South Wilson Avenue, Pasadena, CA 91125.

ometer (PTI), the question of how these stars change in size over their pulsation cycles has been examined in detail. These types of measurements will aid in determining such properties as pulsation mode and nonradial pulsation, basic stellar parameters and, when making narrowband measurements, circumstellar chemistry. The use of nonredundant baselines when taking interferometric measurements may resolve structures on or above the stellar photosphere, such as disks, hot spots, or asymmetric outflows. The spatial geometries of Mira stars, once known, will aid in the physical understanding of what is happening below their photospheres.

Using high-resolution long baseline Michelson interferometry, we present *K*-band observations of asymmetries in the angular diameter of the oxygen-rich Mira variable R Tri. The current work represents the first in a series of papers based on observations of Mira variables using PTI.

2. OBSERVATIONS AND DATA REDUCTION

Observations were made in the *K* band using PTI, as described by Colavita et al. (1999). The data were taken from 2000 October 19–November 19 (JD 2,451,838–2,451,867) and 2001 August 20 (JD 2,452,141) using the northwest baseline (85 m maximum projected). The former time interval spans the visual phases 0.77–0.88, using epoch JD 2,451,633 and a period of 266.4 days as published by Kholopov et al. (1998). The latter date is one period later at visual phase 0.91. The data were calibrated using the standard method as illustrated by Boden et al. (1998). The wideband visibility data is synthesized using the five spectrometer channels across the *K* band, which span the wavelength range 2.0–2.4 μm, yielding an effective bandwidth of 0.097 μm per spectral channel and a resolution ($\lambda/\Delta\lambda$) of $R \simeq 23$ with respect to the center channel at 2.2 μm.

The system visibility—the point-source response of the interferometer—for a given night was measured with respect to two calibration stars, whose small angular sizes are below the resolution limit of the PTI at 85 m and thus are unresolved sources. (For completeness, a $V^2 \geq 0.9$ corresponds to $\leq$1.1 mas for the 85 m baseline in the *K* band.) As stated by Boden et al. (1998), the accuracy of calibrated visibilities is limited by the accuracy and value of the diameter for the calibration objects. The sizes of the calibrators were initially estimated using a blackbody fitted to published photometric data. As such, calibrator sizes were iterated using the data until a consistent solution converged with respect to the target-calibrator pairs for the first night of observations. In this way, the angular diameters of the target and the two calibrators are self-consistent. The solution for the calibrator diameters was then used for all subsequent calibrations in the wideband data (see Table 1). While the measured calibrated size of HD 17573 (B8 Vn) agrees with its bolometric size of 0.62 mas, the calibrated size of HD 14055 (A1 Vnn) is about 20% larger than the expected bolometric fit of 0.60 mas; however, this is comparable to the adopted 0.1 mas uncertainty in sizes.

Error bars on the reduced visibilities of R Tri represent the scatter in the agreement between the two target-calibrator measurements propagated through the binning average; these uncertainties are comparable to the internal scatter of the raw, unbinned visibilities in most cases. Both calibrator sizes were checked for internal consistency on the nights when both were observed and show no change in apparent angular size within the stated uncertainties. Both calibrators were chosen for their proximity to R Tri ($<10^\circ$).

TABLE 1
CALIBRATION STARS

Name	Catalog ID	Spectral Type	m_V (mag)	m_K (mag)	Estimated Diameter[a] (mas)
γ Tri.....	HD 14055	A1 Vnn	4.0	4.0	0.73 ± 0.10
41 Ari...	HD 17573	B8 Vn	3.6	3.8	0.65 ± 0.09

[a] Diameters were fitted to the uniformly bright disk (UD) model.

All apparent angular diameters quoted herein were fitted to the visibility data using a uniform disk model (UD). The predicted visibility for the UD is a function of the projected baseline (B), wavelength of observation (λ), and apparent angular diameter (θ), such that

$$V^2 = \left[2\frac{J_1(\pi\theta B/\lambda)}{(\pi\theta B/\lambda)}\right]^2, \quad (1)$$

where J_1 is the first-order Bessel function.

3. DATA

The wideband normalized visibilities of R Tri, which represent quantities unbiased by any model, are given in Figure 1 for the nine nights of observations and are plotted against spatial frequency. The range of spatial frequencies correspond to observations spanning 40° in position angle at the declination $\delta = 34^\circ.3$. Prominent aspects to these data are noted. First, the data set can be seen as four distinct groups based on the character of their visibility traces in Figure 1 and were binned by hour angle (HA), as given in Table 2. The data in the latter group, P4, were not binned by HA. We have binned the data by HA (0.1 hr bin size, centered at 0.05) in an effort to minimize any artificial structure

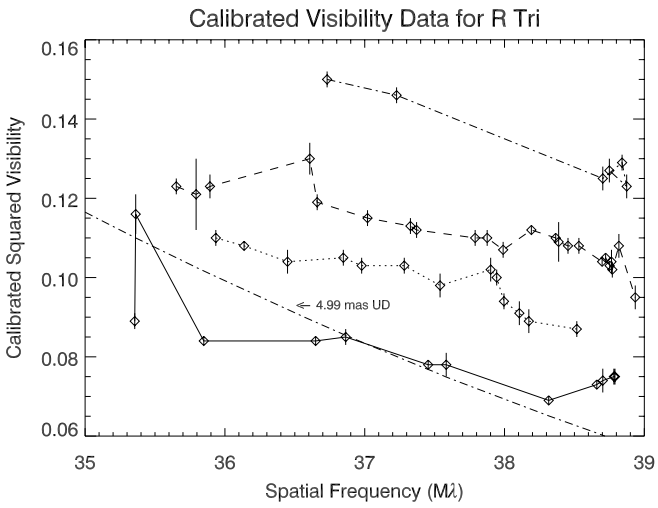

FIG. 1.—Calibrated V^2 data vs. spatial frequency for R Tri. The visibility data traces are, from bottom to top, P1–P4. A spherical UD model of angular diameter 4.99 mas is overlaid for the P1 data, emphasizing the departure from spherical symmetry.

TABLE 2
PTI OBSERVATIONS OF R TRI

Phase Bin Designation[a]	Date	JD 2,400,000 +	P.A. Coverage[b] (deg)
P1	2000 Oct 21	51838	181.6–220.2
P2	2000 Nov 2	51850	183.0–190.0
P2	2000 Nov 3	51851	183.3–194.0
P3	2000 Nov 9	51857	184.7–218.6
P3	2000 Nov 13	51861	186.8–193.6
P2	2000 Nov 14	51862	184.0–189.3
P3	2000 Nov 16	51864	185.7–196.3
P3	2000 Nov 19	51867	182.6–202.4
P4	2001 Aug 20	52141	184.8–201.6

[a] Data binned by visibility trace. See § 3.
[b] Position angles given with respect to north on the sky.

as a result of night-to-night variations within our stated uncertainties. The corresponding spatial frequencies of the HAs are reported herein. Changes in visibility as a function of the spatial frequency are seen when these four groups are viewed as a continuous set of data points. In all groups, the visibilities depart significantly from those of a circular UD. A minimum visibility can be seen for the data taken at phase 0.77 (P1).

Second, an increase in the visibilities (namely, a decrease in the apparent angular diameters) is seen for the phase interval 0.81–0.82, suggesting that R Tri is getting smaller with phases closer to visual maximum. This trend of smaller size continues at phases 0.84–0.88 and can be projected to continue, based on the phase point at 0.91, one period later. Last, on the night of 2000 November 14 (phase 0.86), R Tri appears to have increased in size while maintaining the general characteristics of the shape seen between phases 0.77 and 0.91. An exhaustive search for systematic errors on all the data was conducted, but none were found to dismiss the sudden apparent increase in the size of R Tri for the night in question. Further, an analysis of all the fringe photometric data (stable to about 10%) was conducted, and no sudden brightening could be discerned between the phase intervals 0.86 and 0.90. Since no significant brightening of the source was detected, changes in visibility will correspond to changes in apparent angular size. The sudden 3% apparent size increase at phase 0.86 is, given the calculated uncertainties, a 4 σ event and is likely to be the result of sudden opacity changes in the atmosphere caused by a propagating shock wave. While a second apparent size increase is reflected in Figure 2 at phase 0.88, the likelihood of this being a true "event" is not supported, given the size of the change and uncertainties of the data ($<2\,\sigma$).

On the night of 2000 October 21, contemporaneous data were also taken on the non-Mira giant star HD 15656 (K5 III). These data were calibrated using the same stars as found in Table 1. Spatial coverage of these measurements spanned 41° in position angle, and they were then fitted to a spherical UD fit, which resulted in a χ^2_μ of 0.25. The resultant apparent angular diameter we quote is 2.42 ± 0.04 and agrees to within the uncertainty with a previous measurement of this star at PTI (van Belle et al. 1999).

Given the clear departures from a spherical disk model for R Tri, no attempt is made to correct for limb-darkening effects, such as described by Hofmann, Scholz, & Wood (1998) and van Belle et al. (1996), which result in a correction to the radii of 2%–3%. Given the *K*-band angular sizes, we believe that we are observing the atmosphere of R Tri itself and not a circumstellar shell. Flux contamination by a circumstellar shell is not expected at these wavelengths (Dyck et al. 1992). If the effects seen in the data can be attributed to limb darkening of the photosphere, then the disk in the sphere/disk model would not likely extend beyond the spherical UD in the models; our best-fit models contradict this hypothesis. While we cannot rule out that the changes in visibilities of R Tri could be a result of binary system with this data set, the nature of the angular-size changes from night to night does not support such a conclusion. Additionally, no evidence could be found in the literature to suggest that R Tri has a companion (cf. Belczynski et al. 2000; Mürset & Schmid 1999) that could contribute to the observed visibility changes.

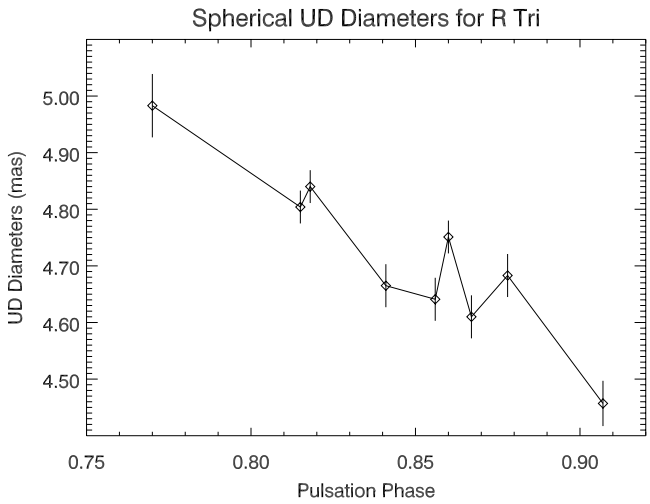

FIG. 2.—Calibrated nightly UD angular diameter data vs. phase for R Tri. A general trend of decreasing angular size with phase toward visual maximum exists, with a sudden increase in size at phase 0.88. Errors are described in § 4.

4. MODELING AND DISCUSSION

Models were constructed by assuming each ellipsoid is uniform in intensity. Where two model geometries overlap, as in the sphere/disk model, the intensities are additive, which is physically correct if the upper layer is optically thin. Each model geometry was then converted to spatial frequencies using Fourier transforms, and the resulting model visibilities as a function of HA were compared against the data set. All modeling was performed using the Interactive Data Language (IDL). We assume face-on geometry in all our models. Figure 2 depicts the best spherical UD model fit, and these results are given as a UD angular size with respect to phase. Each visibility trace in Figure 1 has a uniform slope, but different from that expected from a spherical UD fit at these spatial frequencies. With the exception of the data set at phase 0.91 (one period later), all visibility traces had consistent slopes (UD angular diameter/spatial frequency). Since the slope in the data from phase 0.91 is not consistent with the other data, data from 2001 August 20 were not binned by HA and are reported using the actual spatial frequencies.

TABLE 3
PARAMETERS FOR THE BEST MODEL IN EACH FAMILY OF SIMULATIONS

Shape 1	Phase Bin[a]	a_1	b_1	P.A.$_1$	$(b/a)_1$	Shape 2	a_2	b_2	P.A.$_2$	$(b/a)_2$	I_1/I_2	χ^2_μ
Sphere.....	P1	2.41	...	...	1.00	...	...	...	...	...	...	11.6
	P2	2.41	...	...	1.00	...	...	...	...	...	...	19.8
	P3	2.32	...	...	1.00	...	...	...	...	...	...	32.5
	P4	2.22	...	...	1.00	...	...	...	...	...	...	19.4
Ellipse.....	P1	3.10	2.39	21	0.77	...	...	...	...	...	...	1.49
	P2	3.02	2.16	38	0.72	...	...	...	...	...	...	3.91
	P3	3.17	2.22	27	0.70	...	...	...	...	...	...	3.17
	P4	2.69	2.13	34	0.79	...	...	...	...	...	...	0.69
Sphere.....	P1	2.79	...	...	1.00	Disk	3.34	1.12	22	0.34	0.60	1.15
	P2	3.00	...	...	1.00		3.32	0.73	23	0.22	1.55	4.09
	P3	2.84	...	...	1.00		3.12	0.91	26	0.29	1.24	3.50
	P4	3.02	...	...	1.00		3.18	0.82	24	0.26	1.55	4.10

[a] See Table 2.

Linear fits of spherical UD angular diameters versus spatial frequency were made, and the resulting uncertainties to the fits are given as error bars in Figure 2. In this way, the uncertainties reflect the consistent trend away from the uniform disk model fit and not the changing UD size within each night. For each model, a χ^2_μ was computed for each iteration of size, intensity ratio, and position angle (P.A.) with respect to north on the sky, which is coincident with the semiminor axis. Only models having the lowest χ^2_μ are given in Table 3; however, it must be stressed that the results represent families of plausible models and best-fit solutions to the data set.

Our data suggest that there are at least two families of geometries that fit the data set better than the spherical UD model. For the elliptical model families, P.A.s are consistently between 20° and 35°, with axial ratios ($2b/2a$) between 0.70 and 0.79. These axial ratios are consistent with the ratios seen by other groups on similar stars. In the sphere/disk UD model, a family of spherical stellar atmospheres with angular diameters of the order of ~6 mas, surrounded by a brighter disklike shell of larger length but smaller in width (~1 mas), also fitted the data set better than the spherical UD. Physical parameters and derived quantities for R Tri appear in Table 4; these are based on the averaged model semimajor and semiminor diameters from all phase epochs yielding an effective wideband angular diameter of 5.22 ± 0.30 mas. These uncertainties represent the scatter in the average diameters and are reasonable given the family of models tested. Based on the maximum and minimum visual magnitudes of R Tri and the $V-K$ angular size relation by van Belle (1999), the resultant expected angular size range is 4.5–6.0 mas; the empirical result agrees well with this range of values. This suggests that R Tri is not heavily embedded in dust and its effective temperature of $T_{\rm eff} = 3100$ K is comparable to that of the oxygen-rich Mira models of Bessel et al. (1989). A depiction of the model we adopt, the uniform ellipse, is shown in Figure 3. The best-fit model parameters for the ellipsoids are given in Table 3 along with the derived quantities of the axial ratios.

It should be noted for completeness that a two-layer atmosphere is problematic to model using interferometric data. Scholz (2001) illustrates the point that a two-layer model, especially when applied to very extended atmospheres such as those found in Mira variables, can yield different types of brightness distributions that may have similar "diameter-like" results. The wideband visibilities can be influenced by molecular emission and absorption by species within this band. For these data, the most likely species would include vibrations due to H_2O (1.9 and 2.7 μm) and CO (2.3 μm).

TABLE 4
SOURCE PARAMETERS FOR R TRI (HD 16210)

Parameter	Value	Reference
Spectral type	M4e–M8e	
Visual (mag).....	5.5–12.5	AFOEV data
K band (mag)	1.1	Gezari, Pitts, & Schmitz 1999[a]
Period (day)	266.0	Kholopov et al. 1998
Mean angular diameter[b] (mas).....	5.22 ± 0.30	This work
Bolometric flux (ergs cm^{-2} s^{-1}).....	$(93.3 \pm 9.3) \times 10^{-8}$	Dyck, Lockwood, & Capps 1974[c] at phase 0.11
Effective temperature (K).....	3184 ± 120	$T_{\rm eff} = 2341(F_{\rm bol}/\theta^2)^{1/4}$
Distance (pc).....	350 ± 70	Various sources[d]
Mean linear radius ($R_\odot$)	196 ± 41	This work

[a] Available at CDS, Strasbourg, France, or at http://ircatalog.gsfc.nasa.gov/.
[b] Represents the mean of the major and minor ellipse diameters in Table 3 for the model stellar photosphere.
[c] $T_{\rm eff} = 3000$ K blackbody assumed for spectral types M4–M7.9.
[d] Average of values from Lepine & Paes de Barros 1977: 347 pc; Wyatt & Cahn 1983: 380 pc; Feast & Whitelock 2000: 327 pc. Errors on these values placed at 20%.

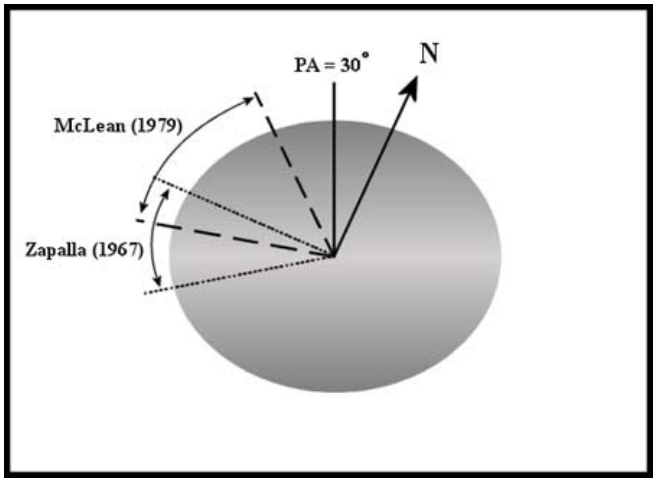

FIG. 3.—Schematic of the elliptical model, with ranges of intrinsic polarization vectors determined by McLean (1979) and Zappala (1967).

Although the CO $\Delta\nu = 2$ band heads lie in the K band, the appreciable number density of H_2O in this oxygen-rich star, in conjunction with the large number of H_2O lines in comparison to CO lines in this photometric band, will cause the H_2O opacity to overwhelm the CO opacity (Alexander, Augason, & Johnson 1989; Brown et al. 1989). If the intensity of emission or absorption of these molecules is strong enough, wideband visibilities can be affected.

There is corollary evidence supporting our nonspherical model found in a study by McLean (1979). He measured that R Tri possesses a moderate level (2%) intrinsic polarization at P.A. $\simeq 60°$ in several discrete bands of TiO, Na I, and Hβ between 4500 and 6000 Å. In the TiO band heads, between 6600 and 7100 Å, the study showed intrinsic polarization at a lower lever ($\simeq$0.5%) varying between P.A. 80° and 110°. Zappala (1967) had shown similar intrinsic polarization in the wideband visible measurements, with roughly consistent P.A.s between 95° and 135°. Usually, scattered light is polarized along the direction perpendicular to the ray from the illuminating source. For a circularly symmetric distribution of scatterers, the net polarization is zero. For an elliptical distribution of scatterers, however, the net polarization would be perpendicular to the semiminor axis. The polarization P.A.s quoted by McLean (1979) and Zappala (1967) are roughly perpendicular to the P.A.s of the model ellipses that fit our data set, suggesting the source of scattering may be coincident to the P.A.s found in our models.

The P.A. of maximum polarization cannot be used indiscriminately to support the ellipse P.A.s quoted in Table 3; studies such as those by Kruszewski, Gehrels, & Serkowski (1968) and McCall & Hough (1980) have shown that polarization P.A.s in long-period variables may not be consistent over time. The source of the short-term polarization variability is unknown. According to Trammell, Dinerstein, & Goodrich (1994), variability in both an intrinsic polarization and P.A. are common in post-AGB stars. In the transition from AGB to planetary nebulae, asymmetries in geometry begin to appear very early. Additionally, evidence for asphericity from their polarization studies can occur in stable as well as time-variable geometries. Tuthill, Hannif, & Baldwin (1999) measured that geometric axial ratios of long-period variables also may not be consistent in value over time.

This suggests that the constituents in the stellar atmosphere of R Tri are sensitive to pulsation phase within the temporal coverage of the data. Hinkle & Barnes (1979) have shown that the majority of the H_2O in the atmosphere of an oxygen-rich Mira variable (R Leo in the study) can exist not only in a circumstellar "warm" region ($T \simeq 1000$ K) about the star, but also at the atmospheric boundary layers (effective temperatures $T_{\rm eff} \simeq 2500$ K). As such, it is reasonable to assume that H_2O is the source of this opacity in R Tri.

Yamamura, de Jung, & Cami (1999) modeled the atmospheres of the Mira variables o Cet and Z Cas using 3–4 μm spectra obtained with the Short Wavelength Spectrometer on the *Infrared Space Observatory*. The models included overlaying a warm molecular region on a 3000 K blackbody. While the models for Z Cas suggested H_2O and SiO molecules would appear only in absorption near pulsation minimum, modeling the spectra for o Cet suggest a region of hot (2000 K) H_2O in emission exists at a distance of $2R_*$, even at pulsation maximum. This is in direct conflict with Hinkle & Barns (1979). We believe rapidly changing opacities may be responsible for what is seen in the geometric models as R Tri approaches pulsation maximum, with H_2O being the dominant opacity source.

Quirrenbach et al. (1992) interpreted their interferometric observations of o Cet as it passed through pulsation maximum as a time-dependent opacity change. In Quirrenbach et al. (1992), the ellipse describing the stellar photosphere changes in size slightly, while the second ellipse, which may be due to a second emitting region near the star, appears to have decreased in size and more so in one direction; thus, the axial ratio has decreased. Assuming that the physical structures represented by both ellipses are located at relatively the same distance from the stellar center, one single event should affect both regions at the same time. An increase in the local density of these regions by impingement of an acoustic shock wave emerging from the photosphere could also explain a change in molecular opacity. In the sphere/disk model, the brighter disk structure increases in intensity significantly from phase 0.77 to 0.84 and gradually fades in intensity thereafter. Coincidentally, this is just before phase 0.85, when the shock is supposed to emanate from the photosphere (Beach, Willson, & Bowen 1988; Bowen 1988). This brighter disk may also be interpreted as a grouping of star spots that, individually, are too small to be resolved but appear to the interferometer as a conglomerate bright region. A bright spot was discovered on α Ori, an M2 supergiant with an extended atmosphere, by Gilliland & Dupree (1996) as observed with the *HST* Faint Object Camera. This bright region was observed by Gray (2000) using coudé spectroscopy ($R = 100,000$) in the visible and is interpreted as an invariant region surrounded by a photosphere that is changing in continuous opacity. Our model results contradict this hypothesis, as the stellar photosphere is changing in size and the brighter region at the stellar equator is changing in both size and intensity.

5. SUMMARY

Visibility data for the Mira variable R Tri departs significantly from a spherically symmetric UD model. This consistent departure is time-dependent between the pulsation phases 0.79 and 0.91, and a general trend of decreasing

angular size exists toward visual maximum. A deviation to this trend appears at pulsation phase 0.86, whereby the UD angular size increases. Models other than the spherical UD were fitted to the data set and resulted in lower χ^2_μ fits as compared to the UD fit. Of the three models tested against the data, either an elliptical UD of axial ratio $(2b/2a) \sim 0.75$ or a spherical UD overlaid with a smaller ellipsoidal disk resulted in the lowest values of χ^2_μ. Each model other than the spherical UD resulted in position angles between 20° and 35°, roughly perpendicular to intrinsic polarization position angles found 30 yr earlier in the optical. These structures may be interpreted as either sources of emission about the stellar photosphere, such as an optically thin disk, or less probably as a grouping of starspots about the photospheric equator.

The observations of R Tri are part of the long-term monitoring program of Mira variables at PTI started in early 1999. The program's goal is to observe changes in apparent angular size with respect to wavelength, pulsation phase, chemical abundance, and strength of acoustic shocks as evidence of pulsation mode.

This work was performed at the Jet Propulsion Laboratory, California Institute of Technology, under contract from the National Aeronautics and Space Administration. Data were obtained at the Palomar Observatory using the NASA Palomar Tested Interferometer, which is supported by NASA contracts to JPL. Science operations with PTI are possible through the efforts of the PTI Collaboration.[5] The authors would like to thank Mel Dyck and Gerard van Belle for their comments, Andy Boden for his help in the analysis of systematics, and Jean Mueller of Palomar Observatory for her efforts in obtaining these data. This research has made use of the SIMBAD and AFOEV databases, operated at CDS, Strasbourg, France.

[5] See http://huey.jpl.nasa.gov/palomar/ptimembers.html.

REFERENCES

Alexander, D. A., Augason, G. C., & Johnson, H. R. 1989, ApJ, 345, 1014
Beach, T. E., Willson, L. A., & Bowen, G. H. 1988, ApJ, 329, 241
Belczynski, K., et al. 2000, A&A, 146, 407
Benson, P. J., et al. 1990, ApJS, 74, 911
Bessell, M. S., Brett, J. M., Scholz, M., & Wood, P. R. 1989, A&AS, 77, 1
Boden, A. F., Colavita, M. M., van Belle, G. T., & Shao, M. 1998, Proc. SPIE, 3350, 872
Bowen, G. H. 1988, ApJ, 329, 299
Brown, J. A., Johnson, H. R., Alexander, D. R., Cutright, L. C., & Sharp, C. M. 1989, ApJS, 71, 623
Castelaz, M. W., Luttermoser, D. G., Caton, D. B., & Piontek, R. A. 2000, AJ, 120, 2627
Colavita, M. M., et al. 1999, ApJ, 510, 505
Dyck, H. M., Benson, J. A., Ridgway, S. T., & Dixon, D. J. 1992, AJ, 104, 1982
Dyck, H. M., Lockwood, G. W., & Capps, R. W. 1974, ApJ, 189, 89
Feast, M. W., & Whitelock, P. A. 2000, MNRAS, 317, 460
Gezari, D. Y., Pitts, P. S., & Schmitz, M. 1999, Catalog of Infrared Observations (5th ed.)
Gilliland, R. L., & Dupree, A. K. 1996, ApJ, 463, L29
Gray, D. F. 2000, ApJ, 532, 487
Hinkle, K. H., & Barnes, T. G. 1979, ApJ, 227, 923
Hofmann, K.-H., Balega, Y., Scholz, M., & Weigelt, G. 2000, A&A, 353, 1016
Hofmann, K.-H., Scholz, M., & Wood, P. R. 1998, A&A, 339, 846
Jura, M. 1994, ApJ, 422, 102
Karovska, M. 1999, in IAU Symp. 191, Asymptotic Giant Branch Stars, ed. T. Le Bertre, A. Lebre, & C. Waelkens (San Francisco: ASP), 139
Kholopov, P. N., et al. 1998, General Catalogue of Variable Stars (4th ed.; Moscow: Nauka)
Kruszewski, A., Gehrels, T., & Serkowski, K. 1968, AJ, 73, 677
Lattanzi, M. G., Munari, U., Whitelock, P. A., & Feast, M. W. 1997, ApJ, 485, 328
Lepine, J. R. D., & Paes de Barros, M. H. 1977, A&A, 56, 219
McCall, A., & Hough, J. H. 1980, A&AS, 42, 141
McLean, I. S. 1979, MNRAS, 186, 21
Mürset, U., & Schmid, H. M. 1999, A&AS, 137, 473
Olnon, F. M., et al. 1986, A&AS, 65, 607
Quirrenbach, A., Mozurkewich, D., Armstrong, J. T., Johnston, K. J., Colavita, M. M., & Shao, M. 1992, A&A, 259, L19
Scholz, M. 2001, MNRAS, 321, 347
Sloan, G. C., & Price, S. D. 1998, ApJS, 119, 141
Trammell, S. R., Dinerstein, H. L., & Goodrich, R. W. 1994, AJ, 108, 984
Tuthill, P. G., Danchi, W. C., Hale, D. S., Monnier, J. D., & Townes, C. H. 2000, ApJ, 534, 907
Tuthill, P. G., Hannif, C. A., & Baldwin, J. E. 1999, MNRAS, 306, 353
Tuthill, P. G., Haniff, C. A., Baldwin, J. E., & Feast, M. W. 1994, MNRAS, 266, 745
van Belle, G. T. 1999, PASP, 111, 1515
van Belle, G. T., Dyck, H. M., Benson, J. A., & Lacasse, M. G. 1996, AJ, 112, 2147
van Belle, G. T., Lane, B. F., Thompson, R. R., & the PTI Collaboration. 1999, AJ, 117, 521
Weiner, J., Danchi, W. C., Hale, D. D., McMahon, J., Townes, C. H., Monnier, J. D., & Tuthill, P. G. 2000, ApJ, 544, 1097
Wyatt, S. P., & Cahn, J. H. 1983, ApJ, 275, 225
Yamamura, I., de Jung, T., & Cami, J. 1999, A&A, 348, L55
Zappala, R. R. 1967, ApJ, 148, L81